Rare Metal Materials and Engineering
Volume 51, Issue 7, July 2022
Available online at www.rmme.ac.cn

Science Press

Cite this article as: Guo Tingbiao, Sun Quanzhen, Li Kaizhe, et al. Effect of Temperature Gradient and Cooling Rate on Solidification Structure and Properties of ZL205A Alloy[J]. Rare Metal Materials and Engineering, 2022, 51(07): 2400-2408.

ARTICLE

Effect of Temperature Gradient and Cooling Rate on Solidification Structure and Properties of ZL205A Alloy

Guo Tingbiao[1,2], Sun Quanzhen[1], Li Kaizhe[1], Huang Dawei[1], Wang Junjie[1], Tai Xiaoyang[1]

[1] State Key Laboratory of Advanced Processing and Recycling of Nonferrous Metals, Lanzhou University of Technology, Lanzhou 730050, China; [2] School of Materials Science and Engineering, Lanzhou University of Technology, Lanzhou 730050, China

Abstract: Due to different influences of cooling rate on the solidification structure of ZL205A alloy under different temperature gradients, the ZL205A alloy with stepped structure of different wall thicknesses was used, and the specimens of different thicknesses were prepared under different solidification conditions. The effects of cooling rate and temperature gradient on solidification structure and tensile strength and elongation of alloys after T5 treatment were explored. In addition, the correlation effect of the phase transformation law with the structure and performance was explored. Results show that the temperature gradient caused by different wall thicknesses have a certain impact on the microstructure and morphology of the alloys. Reducing the temperature gradient can significantly improve the mechanical properties of the alloys. After T5 treatment, the tensile strength of the alloys achieves 506 MPa.

Key words: ZL205A alloy; wall thickness effect; temperature gradient; mechanical properties

The thin-walled ZL205A alloys are widely used in aerospace, long-range missiles, and weapon metallurgy, because of their excellent comprehensive mechanical properties, such as low density, high strength, and good plastic toughness[1] . However, due to the wide difference between the solid and liquid temperatures and the complex composition, ZL205A alloy is difficult to achieve sequential solidification and tends to solidify in a paste state[2,3], which leads to the poor casting performance, great wall thickness sensitivity, and ultimately the mismatch of requirements[4]. The cooling rate and temperature gradient are important process parameters to control the alloy solidification process. Different cooling rates mainly depend on different wall thicknesses of the alloy structure and the heat dissipation performance of the mold. Therefore, in the actual production, the control of the alloy solidification structure is the key to obtain the target alloy with a large difference in wall thickness at different cooling rates[5]. Many complex reactions at different scales are involved in the solidification process of the alloy[6], including the heat transfer, mass transfer, flow on the macroscopic level, and the nucleation and growth of dendrites and eutectic structures on the microscopic level. The dendritic and eutectic structures can influence each other[7]. As the temperature gradient changes regularly, the alloy microstructure undergoes significant changes, thereby affecting the mechanical properties[8]. Bolzoni et al[9] poured the molten alloy into a wedge copper mold and analyzed the effect of cooling rate on the grain size of A356 alloy. It is found that grain size is increased with increasing the cooling rate. Ceschini et al[10] used the metal molds to cast A356 alloy for engine cylinder blocks and cylinder heads, and analyzed the microstructure and mechanical properties of alloys. It is inferred that the grain size has a little effect on the tensile strength of castings, and has a close relationship with elongation and hardness. Jiang et al[11] used A356 alloy to prepare step-structured castings with different wall thicknesses to study the effect of casting wall thickness on the microstructure and mechanical properties of the alloy. It is suggested that as the wall thickness decreases, the refinement degree of the alloy microstructure increases, the grain size and distribution in alloys are improved, and the mechanical properties are also improved. Cao et al[12] studied the solidification structure

Received date: July 20, 2021
Foundation item: Key Science and Technology Research and Development Program of Gansu Province (20YF8GA056); Major Science and Technology Special Project of Gansu Province (1302GKDA015)
Corresponding author: Guo Tingbiao, Ph. D., Associate Professor, School of Materials Science and Engineering, Lanzhou University of Technology, Lanzhou 730050, P. R. China, Tel: 0086-931-2757285, E-mail: 1351462578@qq.com

morphology of silicon in eutectic Al-Si alloy in three types: metal, green sand, and preheated dry sand. It is found that the cooling rate can change the Si morphology in the alloy structure. Zhang et al[13] studied the structure changes of step-shaped Al-Si alloy castings in metal molds, and the results showed that when the alloy is rapidly cooled, the precipitation of Si particles is inhibited, and the coarse structure gradually recovers under slow cooling conditions. Eskin et al[14] studied the influence of cooling rate on the structure formation of Al-Cu alloy, and found the influence of cooling rate on the equilibrium and non-equilibrium phases. ZL205A alloy is a solid solution alloy. When this alloy is solidified, the degree of solidification undercooling is small, therefore restricting its application[15]. The microstructure obtained by solidification process directly affects the alloy properties[16].

In this study, the ZL205A alloy of step structure with different wall thicknesses was used under different conditions. ZL205A alloys with different wall thicknesses were prepared under different cooling conditions, and the effects of solidification conditions, cooling rates, and temperature gradients on the solidification structure and mechanical properties of the alloys were systematically studied. In addition, the phase transformation law of the alloys and the related effects of structure and performance during the solidification process were investigated.

1 Experiment

The step-structured ZL205A alloys were investigated under different conditions: (1) near equilibrium solidification condition I——slow cooling in clay sand molds; (2) near equilibrium solidification condition II——solidification in coated sand molds; (3) high temperature gradient cooling condition III——fast cooling in thick-walled metal molds. The JMatPro software was used to analyze the solidification phase diagrams of ZL205A alloy under high and low temperature gradients, and to simulate the continuous cooling transformation (CCT) curves and isothermal time-temperature-transformation (TTT) curves. The schematic diagrams of the metal molds are shown in Fig. 1. The step-structured metal model in Fig. 1a was buried in the sand box, forming the step structure of sand mold. ZnO was pre-painted on the inner surface of the metal mold, and the mold was preheated to about 150 °C. When the temperature of ZL205A alloy was 730 °C, the molten alloy was poured into the sand molds. The ZL205A alloy was melted in a resistance furnace, and C_2Cl_6 was added. When the temperature was raised to 740 °C, the refining, slagging, and degassing processes were conducted. The molten alloys were separately poured into the step-structured molds with and without ZnO coating with wall thicknesses of 10, 20, 30, 40, and 50 mm. The molten alloy was also poured into the steel mold with different wall thicknesses of 10, 15, 18, 20, and 25 mm. T5 treatment (538 °C/14 h solution+155 °C/8 h aging) was performed on the ZL205A alloy. The alloy specimen was processed into the standard size, and Gatan695 universal electronic tensile testing machine was used to test the mechanical properties at loading rate of 0.5 mm/s. The solution of 99.5vol% H_2O+0.5vol% HF was used to corrode the specimens for 10 s for the microstructure observation by LSM800 optical microscope (OM) and TESCAN MIR A3 scanning electron microscope (SEM). The alloying elements were characterized by the energy disperse spectrometer (EDS).

2 Results and Discussion

2.1 Microstructure of ZL205A alloy under near equilibrium solidification conditions

Fig. 2 shows the microstructures of as-cast alloys in step-structured mold without ZnO coating. The grains have irregular shape with different sizes. The grain boundaries in the as-cast structure are obvious. With the continuous increase of the wall thickness, i. e., with decreasing the temperature gradient, the grains in the alloy gradually grow, and there are a large number of semi-continuous network residual phases at the grain boundaries. The continuous net-like residual phase gradually grows. During the solidification process, the outside part of alloy in contact with the sand mold solidifies firstly, and the temperature is gradually decreased from the outside to the inside of the sand mold. The greater the wall thickness, the longer the solidification time. The grain growth becomes more obvious.

Fig.3 shows the microstructure of as-cast ZL205A alloys in

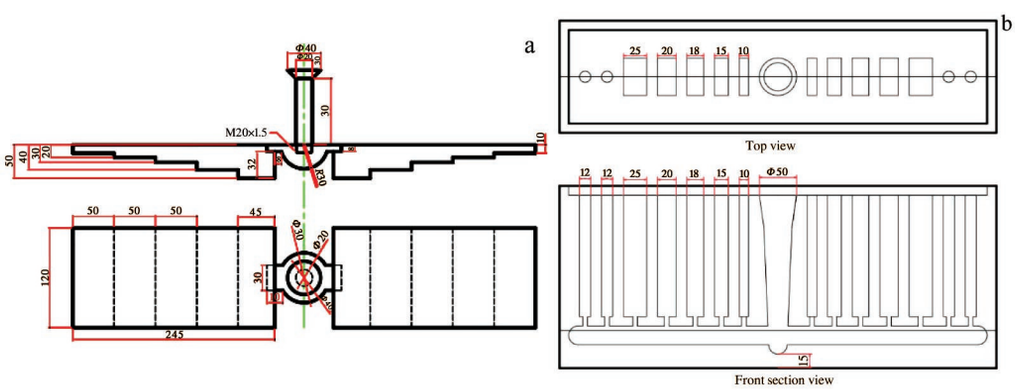

Fig.1 Schematic diagrams of step-structured (a) and steel (b) molds

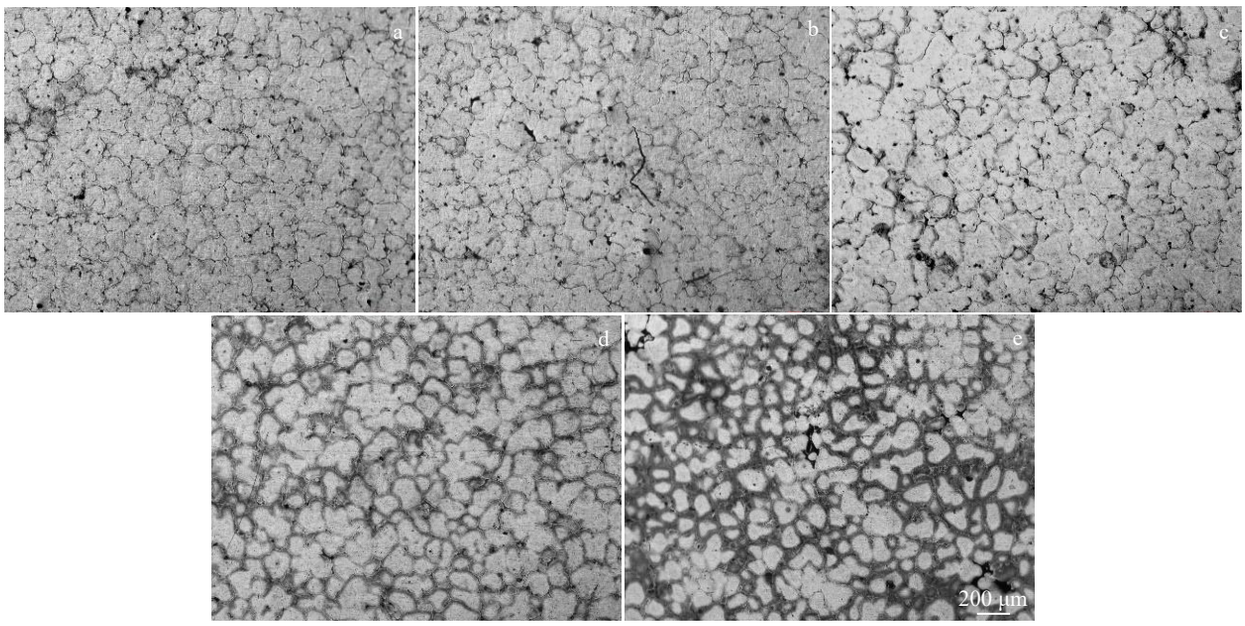

Fig.2 Microstructures of as-cast ZL205A alloy in step-structured mold without ZnO coating at different wall thicknesses: (a) 10 mm, (b) 20 mm, (c) 30 mm, (d) 40 mm, and (e) 50 mm

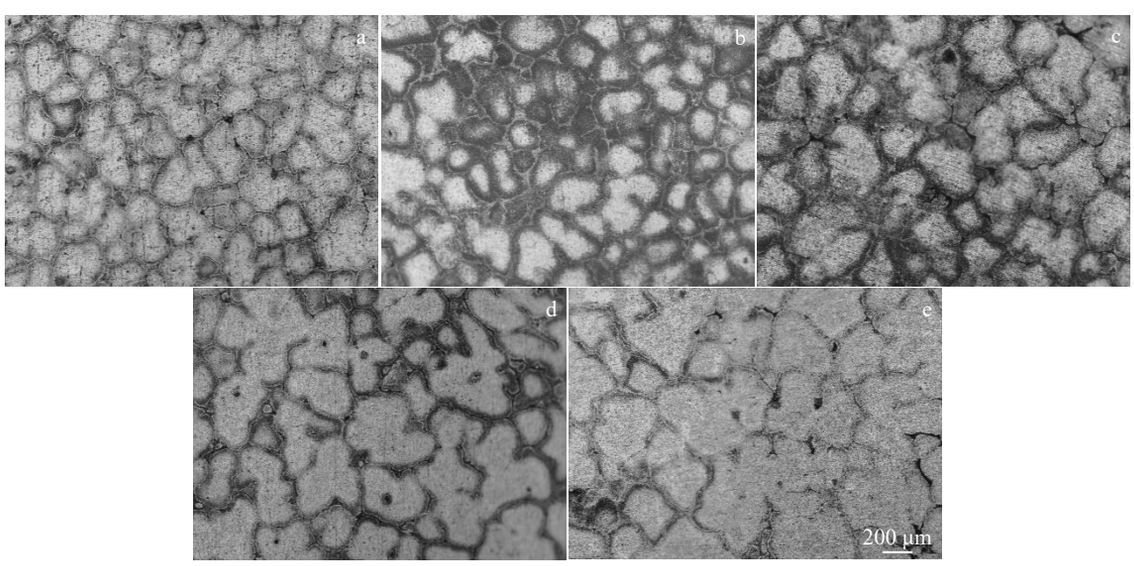

Fig.3 Microstructures of as-cast ZL205A alloy in step-structured mold with ZnO coating at different wall thicknesses: (a) 10 mm, (b) 20 mm, (c) 30 mm, (d) 40 mm, and (e) 50 mm

the step-structured mold with ZnO coating at different wall thicknesses. Similarly, as the temperature gradient decreases, i. e., as the wall thickness increases, the alloy microstructure becomes coarse, and the grains gradually increase. The dendrites and grains are obviously coarser, the pores shrink at the thick-walled area, and the structure is uncompacted. The grain boundaries of the alloy with wall thickness of 50 mm are thicker than those with thin wall thickness. Thus, the loose pinholes, concentrated low-melting compounds, and concentrated defects are easily produced at the grain boundary. The grain connection is less tight. The grains and dendrites at the thin wall are obviously smaller, and the overall structure is more uniform than that at the thick wall. Because the cooling rate of the molten metal is greater at the thin wall, the solidification duration is shorter, especially for the solid solution alloys. Meanwhile, the contact between the molten ZL205A alloy and the mold produces a strong heat exchange, which leads to different microstructures of the alloy.

Fig.4 shows the microstructures and EDS spectra of the as-cast ZL205A alloy in the step-structured mold without ZnO

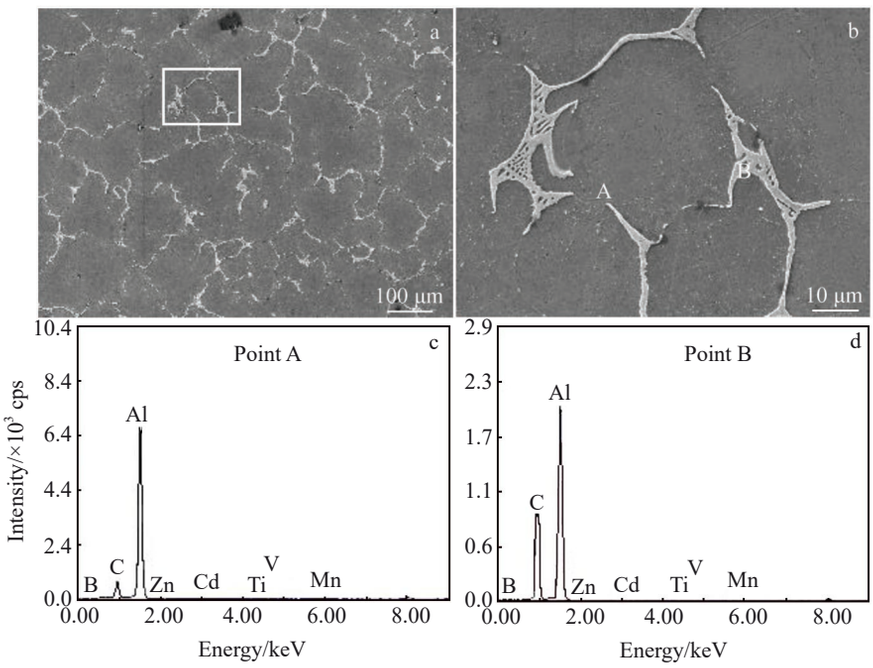

Fig.4 SEM microstructure of as-cast ZL205A alloy in step-structured mold without ZnO coating (a); magnified microstructure of rectangular area in Fig.4a (b); EDS spectra of point A (c) and point B (d) in Fig.4b

coating. It can be clearly seen that the microstructure has clear grain boundaries, the grains mainly have irregular ellipse shape, but the size of the grains is not uniform. The black matrix phase and the white network phase at the grain boundary are investigated through EDS spectra of the as-cast ZL205A alloy. According to Fig. 4c and 4d, the black matrix phase is α-Al, and the white network phase at the grain boundary is the Al_2Cu secondary phase. The secondary phase has an uneven distribution, and its length is different with wide grain boundaries. There are a series of discontinuous network components at the grain boundaries. The α-Al and Al_2Cu exist between the dendrites and at the grain boundary, thereby forming the eutectic structure.

2.2 Microstructure of ZL205A alloy under high temperature gradient

Fig. 5 shows the microstructure of the as-cast ZL205A alloy in steel mold under different temperature gradients when the pouring temperature is 730 °C. As the temperature gradient decreases, the grain size gradually increases, and the width of the white phase distributed along the grain boundary becomes smaller. The grains in the alloy are approximately equiaxed and relatively coarse. The distribution of precipitation phase at the grain boundary is discontinuous. In Fig. 5a~5c, the white phase is relatively thick. In Fig. 5d and 5e, the white phase is transformed into the elongated strips. In Fig. 5e, there are some long strips of the white phase. The phases are obviously fused, forming short rods or granules, and the distribution of crystal grains becomes more homogenous.

According to Fig. 6, in the as-cast ZL205A alloy, Cu atoms are mainly concentrated near the grain boundary in the form of θ phase. The α-Al exists on the grain boundary and Al_2Cu is precipitated by the eutectic reaction, forming the eutectic structure. Al_2Cu is distributed at the grain boundary in the irregular network and strip shape, and a small amount of Al_2Cu exists inside the crystal grain in a granular shape.

2.3 Mechanical properties

2.3.1 Mechanical properties of ZL205A alloys under low temperature gradients

Table 1 shows the tensile strength and elongation of ZL205A alloy in the step-structured molds with and without ZnO coating under different temperature gradients. The highest tensile strength of the alloy in the step-structured mold without ZnO coating at wall thickness of 10 mm is 176 MPa, and that with ZnO coating at the same wall thickness is 159 MPa. With the wall thickness of 50 mm, the tensile strength of alloys is low, reaching only 107 and 105 MPa when the alloys are solidified in step-structured molds without and with ZnO coating, respectively, which can be attributed to the fact that when the alloy wall is too thick, the heat cannot be quickly dissipated. The longer solidification duration provides sufficient time for grain growth, which leads to the formation of relatively longer grains and more defects, such as thermal cracking and pore shrinkage. Therefore, the mechanical properties of alloys at thick wall thickness are inferior, and they have a great relationship with the temperature gradient. The tensile strength of the alloys in the step-structured mold without ZnO coating is generally higher than that with ZnO coating at the same wall thickness, because the thermal conductivity and heat transfer of the step-structured mold without ZnO coating are better than those with the ZnO coating.

The elongation of the ZL205A alloy is only 4.6% and 7.6%

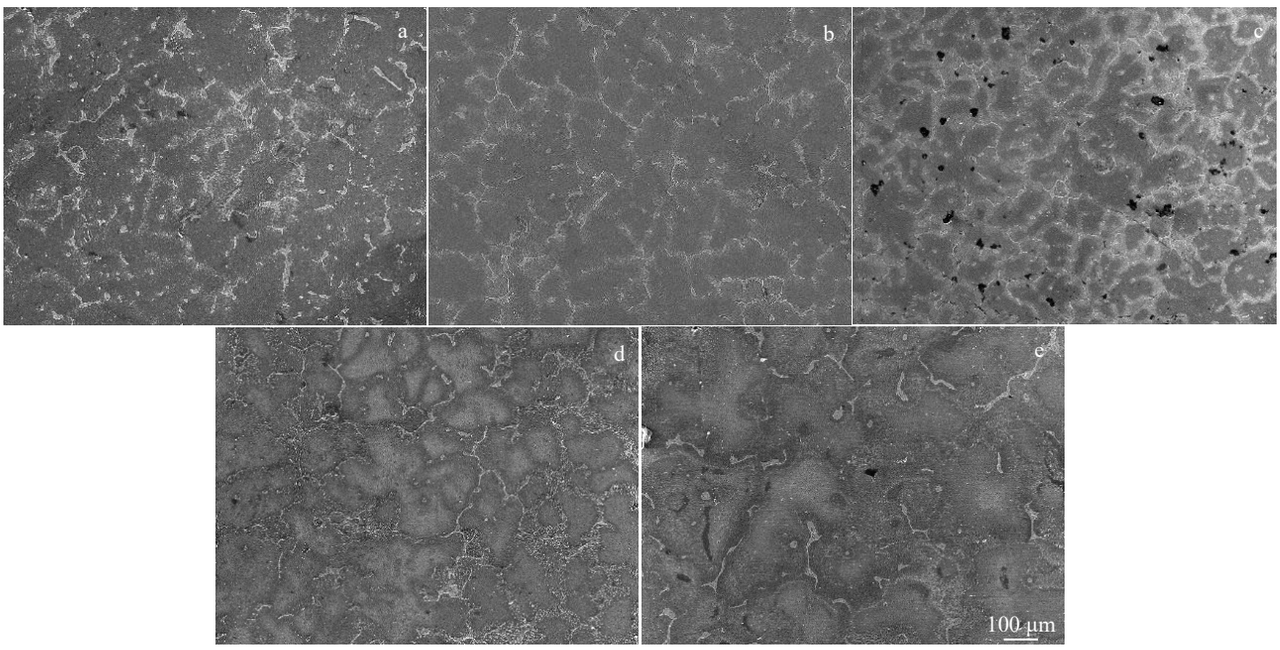

Fig.5 Microstructures of as-cast ZL205A alloy in steel mold at different wall thicknesses: (a) 10 mm, (b) 15 mm, (c) 18 mm, (d) 20 mm, and (e) 25 mm

in step-structured molds without and with ZnO coating at wall thickness of 10 mm, respectively. The highest elongation of the as-cast alloy of 10.9% is achieved when it is solidified in the step-structured mold with ZnO coating at wall thickness of 50 mm. Compared with that in the step-structured mold without ZnO coating, the elongation is increased by 13.5%, which is mainly due to different cooling rates caused by the difference in heat storage capacity and heat transfer property of different molds. Because of different temperature field distributions during the pouring process and the solidification process, different structures appear, which directly affects the elongation of the alloys. It can be concluded that the elongation of the alloys is more sensitive to the defects in the alloy microstructure.

2.3.2 Mechanical properties of alloys under high temperature gradients

Fig.7 shows the stress-strain curves of ZL205A alloy under the high temperature gradients (solidification in steel mold). As the wall thickness increases, the curve gradually moves downwards, and the tensile strength of the alloy becomes smaller. The smaller the wall thickness, the higher the tensile strength. Table 2 shows the tensile strength and elongation of

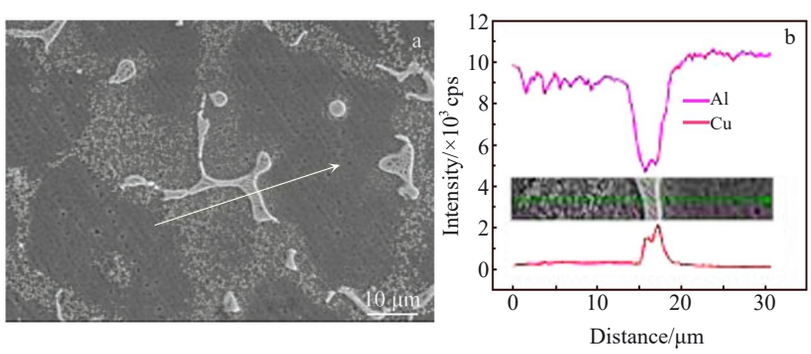

Fig.6 SEM microstructure of white phase in ZL205A alloy in steel mold (a) and EDS line scanning along arrow line (b)

Table 1 Tensile strength and elongation of ZL205A alloys in step-structured molds with and without ZnO coating at different wall thicknesses

Step-structured mold	Tensile strength/MPa					Elongation/%				
	10 mm	20 mm	30 mm	40 mm	50 mm	10 mm	20 mm	30 mm	40 mm	50 mm
Without ZnO coating	176	174	169	141	107	4.6	7.3	8.2	8.7	9.6
With ZnO coating	159	134	130	126	105	7.6	8.7	9.1	10.0	10.9

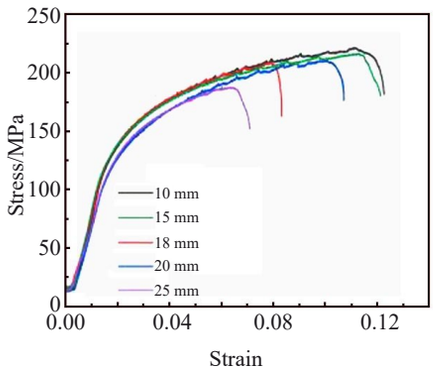

Fig.7 Stress-strain curves of ZL205A alloys in steel mold at different wall thicknesses

Table 2 Tensile strength and elongation of ZL205A alloy in steel mold at different wall thicknesses

Wall thickness/mm	10	15	18	20	25
Tensile strength/MPa	219	217	210	208	187
Elongation/%	12.1	11.2	9.8	7.8	6.2

the alloy at the high temperature gradients. The tensile strength of the alloy at the wall thickness of 10 mm reaches a peak value of 219 MPa, which is 24.4% higher than that of the alloy solidified in the step-structured mold without ZnO coating at wall thickness of 10 mm. With the wall thickness of 25 mm, the tensile strength is low, reaching only 187 MPa. In general, the mechanical properties of alloy in steel mold are better than those in the step-structured mold. The alloy temperature gradient is large, the heat dissipation rate during solidification and cooling is slow, and the solidification duration also lengthens, leading to longer time for internal grain growth. Besides, the material has many defects, resulting in inferior mechanical properties of alloys. The temperature gradient and cooling rate have a great impact on the mechanical properties of the ZL205A alloys.

2.4 Thermodynamic phase diagram calculation

Fig. 8 shows the equilibriumand and non-equilibrium solidification phase diagrams of ZL205A alloy calculated by JMatPro thermodynamics software. It can be seen that the phase components of the alloy are Al, Al_2Cu, and $Al_{20}Cu_2Mn_3$. The liquidus temperature of the alloy is 656.9 °C. The Al phase begins to precipitate during the cooling process, and then the $Al_{20}Cu_2Mn_3$ phase is gradually precipitated. The solidus temperature of the alloy is 555.2 °C. When the temperature decreases to 533.8 °C, Al_2Cu phase forms in the alloy, and its precipitation amount is 6.18mol% at 100 °C. Therefore, the equilibrium phase components of ZL205A alloy at room temperature (the content of components barely changes below 100 °C) are 92.13mol% Al, 6.18mol% Al_2Cu, and 1.69mol% $Al_{20}Cu_2Mn_3$. Fig. 8b shows the non-equilibrium solidification process curves of ZL205A alloy. It can be seen that during the alloy solidification, Al, Al_2Cu, and $Al_{20}Cu_2Mn_3$ phases are precipitated in sequence, and the phase content

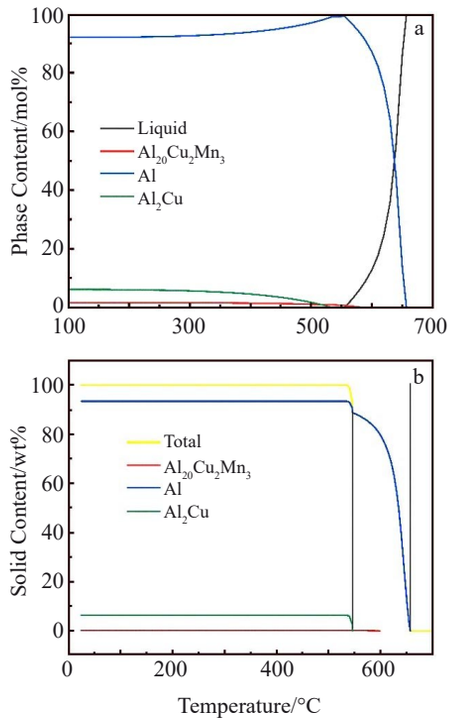

Fig.8 Simulated equilibrium (a) and non-equilibrium (b) solidification phase diagrams of ZL205A alloy

tends to be stable. Due to the incomplete diffusion of elements, the phase content is different from that during the equilibrium solidification. The phase components are 93.5wt% Al, 6.4wt% Al_2Cu, and 0.14wt% $Al_{20}Cu_2Mn_3$. The Gibbs free energy minimization principle is used in this calculation.

The TTT and CCT curves of the alloy are calculated by JMatPro software. The Johnson-Mehl-Avrami (JMA) phase transition kinetic equation, nucleation rate, wetting angle, diffusion coefficient, and growth rate can be expressed by Eq.(1~5), respectively, as follows:

$$x = \frac{V}{V_{eq}(T)} = 1 - \exp\left(-\frac{\pi}{3} N_r G_r^3 t^4\right) \quad (1)$$

$$N_r = \frac{ND_{eff}}{a_0^2} \exp\left(-\frac{16\pi\alpha^3}{3NkT} f(\theta) \frac{\Delta H_m^3}{\Delta G_m^2}\right) \quad (2)$$

$$f(\theta) = (2 - 3\cos\theta + \cos^3\theta)/4 \quad (3)$$

$$D_{eff} = D_0 \exp(D_{eff}/RT) \quad (4)$$

$$G_r = kD_{eff}\left(\frac{\Delta G_m}{RT}\right) \quad (5)$$

where x is the new phase transition variable; V is the volume fraction of the new phase transition at a certain temperature for a certain period; $V_{eq}(T)$ is the total amount of the new phase in the equilibrium state at a certain temperature for a certain period; N_r is the nucleation rate; G_r is the growth rate; t is the phase transition incubation period; N is the nucleation number; a_0 is the distance between particles; α is the nucleus radius; k is the Boltzmann constant; T is absolute temperature; ΔH_m is the enthalpy change; ΔG_m is the growth driving force;

θ is the wetting angle; D_{eff} is the diffusion coefficient; D_0 is the diffusion constant; R is gas constant.

Fig.9a and 9b show the TTT and CCT curves obtained from the heat treatment process of ZL205A alloys, respectively. It can be seen that the TTT curve of each phase in the alloy is in the C shape, because the high degree of undercooling at low temperature is conducive to the nucleation of the precipitated phase, but the element diffusion effect is slight and the grain growth is slow. The nucleation is difficult but the element diffusion is easy at high temperature. Therefore, the phase precipitation (GP) speed is relatively fast at the medium temperature, and the incubation time is short. The specific temperature of θ' phase, GP zone, and Al_2Cu phase is 180, 360, and 450 °C respectively. The incubation time of Al_2Cu phase (243.6 s) is longer than that of GP zone and θ' phase. Fig. 9b shows CCT curves obtained during the T5 heat treatment of the ZL205A alloys. The faster the cooling rate, the more difficult the phase formation. When the cooling rate is relatively slow, GP zone, θ' phase, and Al_2Cu phase all tend to precipitate, because the slower the cooling rate, the more obvious the element diffusion effect, the easier the phase precipitation. Therefore, by controlling the cooling rate, the precipitation of each phase can be suppressed, and a supersaturated solid solution can be obtained.

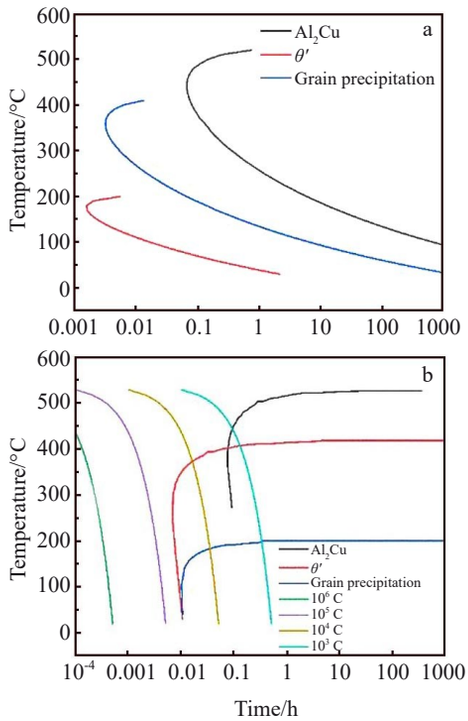

Fig.9 TTT (a) and CCT (b) curves of ZL205A alloys during T5 heat treatment

2.5 Structure and properties of ZL205A alloys after T5 treatment

Fig. 10 shows the microstructures of the ZL205A alloys under the high temperature gradients after T5 treatment, which show the approximately equiaxed crystal shape. Most θ phase is concentrated at the intersection of multiple grain boundaries. The grains are arranged tightly, and there is a black phase in the grains and the Al solid solution. After T5 treatment, the grain boundary width is increased, and the grain boundary shows network shape and is semi-continuously distributed. The precipitated phases are greatly reduced, existing in the form of strip or fishbone. In addition, the granulation occurs, and the crystal grains are tightly arranged.

Fig.11 shows the stress-strain curves of ZL205A alloys after T5 treatment. After heat treatment, the mechanical properties of the alloy are further improved due to the aging

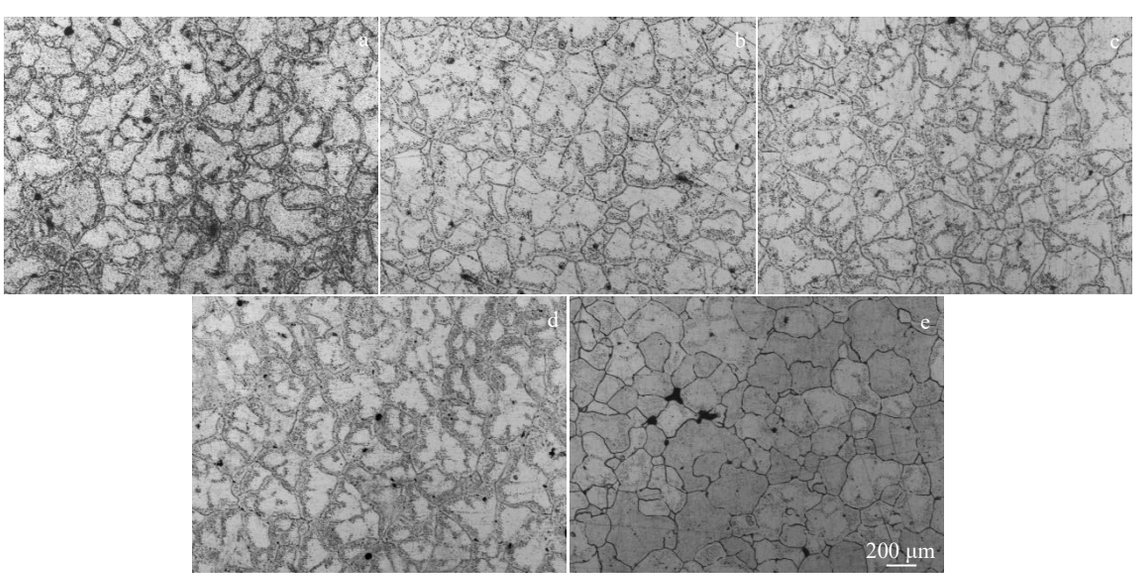

Fig.10 Microstructures of ZL205A alloys solidified in steel mold after T5 heat treatment at different wall thicknesses: (a) 10 mm, (b) 15 mm, (c) 18 mm, (d) 20 mm, and (e) 25 mm

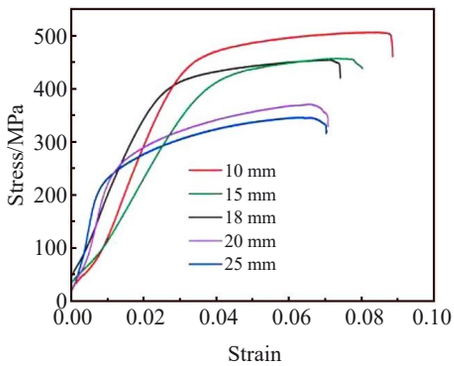

Fig.11 Stress-strain curves of ZL205A alloys in steel mold at different wall thicknesses after T5 heat treatment

Table 3 Tensile strength of ZL205A alloys in steel mold at different wall thicknesses after T5 heat treatment

Wall thickness/mm	10	15	18	20	25
Tensile strength/MPa	506	457	455	371	346

strengthening effect. The tensile strength of the alloy at the wall thickness of 10 mm exceeds 500 MPa, which is almost 2.5 times higher than that of the as-cast alloy under the same conditions.

Table 3 shows the tensile strength of ZL205A alloys after T5 treatment. The tensile strength of alloy at the wall thickness of 10 mm reaches 506 MPa, and that at the wall thickness of 25 mm is 346 MPa. In the T5 treatment, the supersaturated solid solution decomposes and the crystalline lattice of the alloy matrix is greatly restored. In a stable state, the elements in the alloy begin to diffuse freely to fill the vacancies formed by quenching. Because ZL205A alloy contains many elements, the complex effects and restrictions may occur during the heat treatment, and the heat treatment process has a significant effect on the evolution of the internal microstructure of the alloy.

3 Conclusions

1) The cooling rate and temperature gradient caused by the mold and wall thickness have a great impact on the microstructure of the ZL205A alloys. The thicker the wall, the larger the grain size and the more inferior the mechanical properties of alloys. The mechanical properties of alloys solidified in the metal mold are generally higher than those in the step-structured mold.

2) When the ZL205A alloy approaches the equilibrium solidification, the phase components are Al, Al_2Cu, and $Al_{20}Cu_2Mn_3$, the liquidus temperature is 656.9 °C, and the solidus temperature is 555.2 °C. When the temperature drops to 533.8 °C, Al_2Cu phase forms in the alloy. The equilibrium phase components at room temperature are 92.13mol% Al, 6.18mol% Al_2Cu, and 1.69mol% $Al_{20}Cu_2Mn_3$. When the alloy is in the non-equilibrium solidification, the phase components at room temperature are 93.5wt% Al, 6.4wt% Al_2Cu, and 0.14wt% $Al_{20}Cu_2Mn_3$. Al, Al_2Cu, and $Al_{20}Cu_2Mn_3$ phases are precipitated in sequence.

3) After T5 treatment of the alloys formed under a high temperature gradient, the grain boundary width is increased. The semi-continuously distributed network precipitated phases at the grain boundary are greatly reduced, and the mechanical properties of alloys are significantly improved. The tensile strength at the wall thickness of 10 mm exceeds 500 MPa.

References

1 Deng Yunlai, Zhang Xinming. *The Chinese Journal of Nonferrous Metals*[J], 2019, 29(9): 2115 (in Chinese)
2 Cheng Yunchao, Yang Guangyu, Lv Sanlei *et al*. *Foundry*[J], 2014, 63(1): 10 (in Chinese)
3 Xu Chao, Zhao Junwen, Luo Qinglin *et al*. *Rare Metal Materials and Engineering*[J], 2016, 45(6): 1559 (in Chinese)
4 Zhao Lihong, Bi Tao. *Special Casting & Nonferrous Alloys*[J], 2011, 31(3): 226 (in Chinese)
5 Chen Rui. *Thesis for Master*[D]. Beijing: Tsinghua University, 2017 (in Chinese)
6 Yan Weidong. *Thesis for Master*[D]. Xi'an: Northwestern Polytechnical University, 2002 (in Chinese)
7 Liu Feng, Wang Haifeng, Song Shaojie *et al*. *Progress in Physics* [J], 2012, 32(2): 57
8 Bao Xiaodong. *Thesis for Master*[D]. Hefei: Anhui University of Technology, 2014 (in Chinese)
9 Bolzoni L, Babu N H. *Journal of Materials Processing Technology*[J], 2015, 222: 219
10 Ceschini L, Morri A, Morri A *et al*. *Materials & Design*[J], 2011, 32(3): 1367
11 Jiang W M, Fan Z T, Chen X *et al*. *Materials Science & Engineering A*[J], 2014, 619: 228
12 Cao Liyun, Liu Xingjiang, Yang Xiaoping *et al*. *Journal of Liaoning Institute of Technology*[J], 2001, 21(4): 42 (in Chinese)
13 Zhang Rong, Shen Shujuan, Zhao Zhilong *et al*. *Nonferrous Metals*[J], 2002, 54(3): 20 (in Chinese)
14 Eskin D, Du Q, Ruvalcaba D *et al*. *Materials Science & Engineering A*[J], 2005, 405(1-2): 1
15 Deng Panke, Yang Zhiyong, Han Jianmin *et al*. *Casting*[J], 2019, 68(12): 1368 (in Chinese)
16 Chen Junyu, Qiu Zhesheng, Li Jiaqi *et al*. *Rare Metal Materials and Engineering*[J], 2020, 49(9): 2966

温度梯度和冷却速率对ZL205A合金凝固组织及性能的影响

郭廷彪[1,2]，孙全珍[1]，李凯哲[1]，黄大伟[1]，王俊杰[1]，郃晓阳[1]

(1. 兰州理工大学 省部共建有色金属先进加工与再利用国家重点实验室，甘肃 兰州 730050)

(2. 兰州理工大学 材料科学与工程学院，甘肃 兰州 730050)

摘　要：由于在不同温度梯度下ZL205A合金冷却速率对凝固组织的影响不同，采用不同壁厚的阶梯状结构的合金，在不同凝固条件下制备厚度不同的合金试样，探究了冷却速率及温度梯度对合金凝固组织及T5处理后合金抗拉伸强度及延伸率的影响，同时探索了合金的相变规律与组织和性能的关联效应。实验结果表明：由壁厚差引起的温度梯度对合金的微观组织及形貌会产生一定的影响，降低温度梯度的合金力学性能显著提升，T5处理后合金的抗拉伸强度达到506 MPa。

关键词：ZL205A合金；壁厚效应；温度梯度；力学性能

作者简介：郭廷彪，男，1974年生，博士，副教授，兰州理工大学材料科学与工程学院，甘肃 兰州 730050，电话：0931-2757285，E-mail：1351462578@qq.com